BRIDGE WINDSHIELD DESIGN TO AVOID AEROELASTIC PHENOMENA

Mikel Ogueta-Gutiérrez
Instituto Universitario de Microgravedad Ignacio da Riva.
Universidad Politécnica de Madrid
Plaza Cardenal Cisneros, s/n
28040 Madrid, Spain
mikel.ogueta@upm.es

Sebastián Franchini
Instituto Universitario de Microgravedad Ignacio da Riva.
Universidad Politécnica de Madrid
Plaza Cardenal Cisneros, s/n
28040 Madrid, Spain
s.franchini@upm.es

KEYWORDS: bridge design, aeroelastic, flutter, VIV

ABSTRACT

Since in 1940 the Tacoma Narrows Bridge was destroyed by the wind, aeroelastic instabilities have been recognized as one of the most challenging aspects of bridge design. They can produce long-term fatigue failure through vortex induced vibrations, or sudden collapse through self-excited flutter. These vibrations may also cause discomfort for the users and temporary closure of the bridge.

Wind tunnel studies are a very helpful tool to understand these phenomena. By means of them, the critical wind speed at which vortex induced vibration and flutter appear can be precisely determined and the design of the bridge can be reconsidered in the early steps of the process.

In this paper, an optimum design of the bridge section is sought. One of the most relevant parameters that influence the stability of a certain deck is the porosity of the barriers. Section model tests have been carried out to find whether an optimum value of the porosity of the barrier exists. This value or range of values must present neither vortex induced vibration nor flutter.

INTRODUCTION

Slender structures such as skyscrapers and bridges are becoming more and more slender and light. This trend brings a side effect: their natural frequencies are becoming smaller, and therefore, they are turning more wind-sensitive. Submerged in a wind current, bridges can suffer low-frequency vibrations. These vibrations can be mainly divided in two: on the one hand, vortex induced vibrations (VIV) are bounded and limited to a narrow range of velocities. On the other hand, flutter is an unbounded phenomena that can lead to the collapse of the bridge, as happened to the Tacoma Narrows Bridge in November 1940 (Masaru Matsumoto et al. 2003).

VIV cannot destroy the bridge, but it can introduce heavy fatigue loads on the bridge or in several slender elements of it such as cables or hangers (Cluni et al. 2007; Chen et al. 2012). The failure of these elements can produce the collapse of the bridge, and even if that point is not reached, maintenance operations would increase their cost notably. The physical phenomenon underlying this vibration is the

periodic shedding of vortices from bluff bodies. When the frequency of the vortices shed in the wake of the slender element match its natural frequency, vibration is triggered. For a narrow range of velocities, the shedding frequency of vortices is not led by the wind velocity but by the movement of the bridge itself. This phenomenon is called lock-in. Some more information about VIV can be seen elsewhere (Simiu & Robert H. Scanlan 1996; M. Matsumoto 1999).

The mechanisms of flutter are more complex and are less understood. At a certain wind velocity, the movement of the bridge in the current alters its dynamic properties, and the overall damping (structural damping plus aerodynamic damping) vanishes. Therefore, the bridge starts to vibrate in an uncontrolled and unbounded manner until its collapse if the wind speed is maintained. After the Tacoma Narrows event, the focus has been put in the prevention of this instability. Some designers have focused on the development of dampers (either active or passive) to reduce the amplitude of vibration (Kobayashi & Nagaoka 1992; Aslan & Starossek 2008). Others, on the other hand, have pointed out the key role of a good section design. Several papers have underlined the importance of even small details in the stability of bridges (Jones et al. 1995; Yoshimura et al. 1997). For the determination of the critical wind speed at which flutter appears and to evaluate the goodness of a certain configuration, wind tunnel tests are one of the most useful and complete tool.

In this paper, ambient vibration tests have been performed on a bridge section varying the porosity of the barrier to study the effect of this parameter in the stability of the whole system. The next section is devoted to describe the setup of the tests. The results section sums up the main findings. Finally, the conclusions are extracted and enumerated.

SETUP

The selected bridge section for these tests is the Anaklia footbridge project. The section of this footbridge can be seen in figure 1. The main dimensions of this bridge, besides the dynamic properties, are shown in table 1.

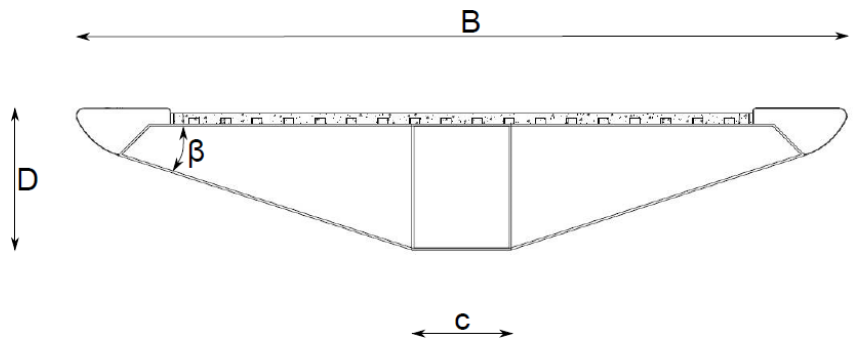

Figure 1. Section of the tested footbridge. Main dimensions are given in table 1

Magnitude (units)	Symbol	Value
Length (m)	L	1.05
Width (m)	B	0.186
Height (m)	D	0.035
Soffit width (m)	c	0.02375
Angle of the bridge (º)	β	18
Linear mass (kg/m)	m	1.8
Mass moment of inertia (kg·m^2/m)	I	0.03
Bending frequency (Hz)	f_h	4.05
Torsional frequency (Hz)	f_α	5.05
Bending damping (%)	δ_h	0.025
Torsional damping (%)	δ_α	0.025

Table 1. Main dimensions and dynamic properties of the section tested

The setup for the tests can be seen in figure2. In order to measure the velocity of the wind, a hot-wire anemometer is placed upstream the model.

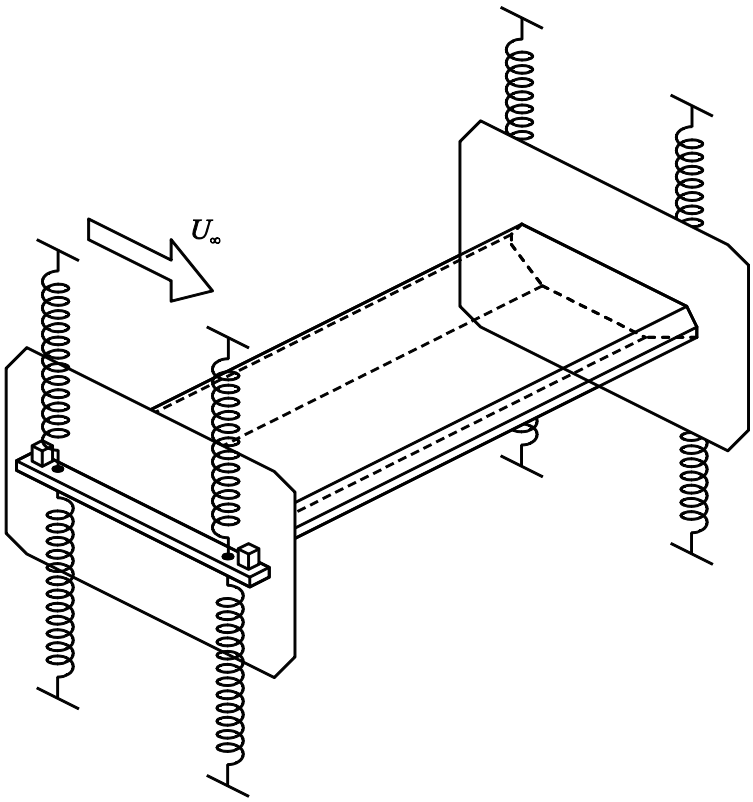

Figure 2. Setup for the tests. The bridge section model is hung from springs that reproduce the elastic properties of the prototype

The displacement is measured via two laser devices that deliver distance to the bridge. As they are placed, their semi-sum gives the displacement of the centreline, whilst its difference divided by the space between the lasers gives the torsional angle in radians (assuming small values of the torsion). The procedure for the tests is simple. The wind tunnel is set to a constant velocity. When the flow is stabilized, the measurements of the lasers and the hot wire are recorded for 20 seconds at a sampling frequency of 1000 Hz. After that, the velocity is increased, and the process, repeated. When flutter condition is reached, this process should be taken carefully, since the risk of breakage of the model exists. If the amplitude (either in bending motion or in torsion) is too high, the test must be immediately stopped.

The wind tunnel used for this campaign is the A9 wind tunnel in the Instituto Universitario de Microgravedad Ignacio da Riva, IDR¨/UPM. It is an Eiffel type wind tunnel driven by 9 fans. A sketch of it can be seen in figure 3. The size of the test chamber is 1.8 metres high and 1.5 metres wide. Upstream the test chamber, a screen has been placed to reduce the turbulence. The measured free stream turbulence is between 2 and 2.5%.

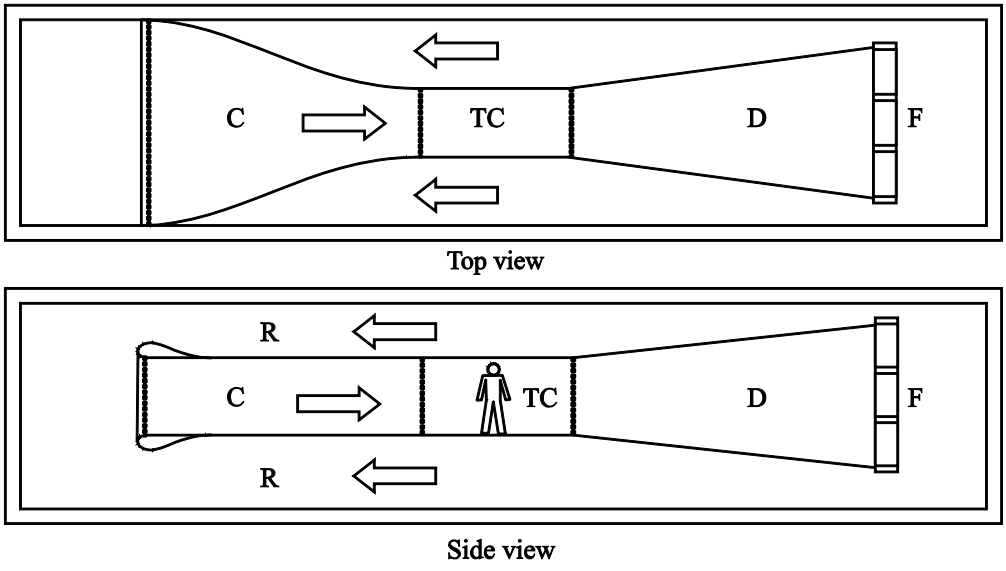

Figure 3. Sketch of the A9 wind tunnel in IDR/UPM. TC is the test chamber, D the diffuser, F the fans, R the return circuit, and C the contraction.

RESULTS

8 different barrier configurations have been tested. The reference barrier is a 5 cm high barrier, composed of 5 wood sticks of a height of 5 mm spaced 5 mm between them. This is the most porous barrier among the ones tested. On the other hand, the limit is set by the solid barrier, where the reference barrier is totally covered. In between, other six configurations have been created by uncovering parts of the solid barrier. The code for all the barriers and a small description is available in table 2.

Code	Description
Ref	Reference barrier
25cm	25 cm gap every 30 cm
20cm	20 cm gap every 30 cm
15cm	15 cm gap every 30 cm
5cm	5 cm gap every 30 cm
3cm	3 cm gap every 30 cm
1cm	1 cm gap every 30 cm
Solid	Barrier totally covered

Table 2. Tested configurations

To make clearer, in figure 4, configuration 3cm can be seen. The gap is 3 mm wide and there are gaps every 30 cm.

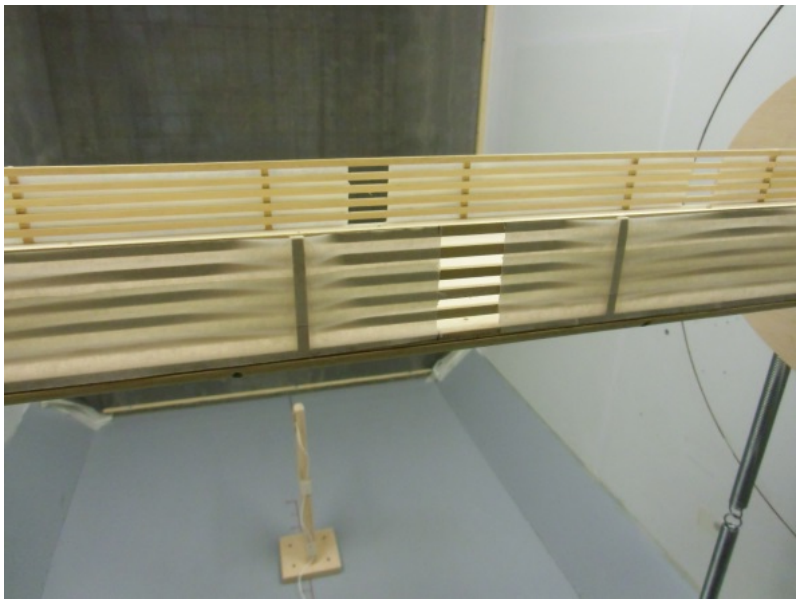

Figure 4. Configuration 3cm placed in the wind tunnel. The support for the hot wire can be seen in the lower part. Upstream, the grid for reduction of the turbulence is placed.

For the sake of clarity, the results are plotted in two different graphs. In the first one, figure 5, the most "covered" barriers can be seen (from the 15cm configuration to the solid one). In that figure, the root mean square (RMS) value of the bending time series and the torsion time series can be seen. The bending RMS value is made dimensionless with the thickness of the deck. They are both plotted against the reduced velocity, $U_R = U$

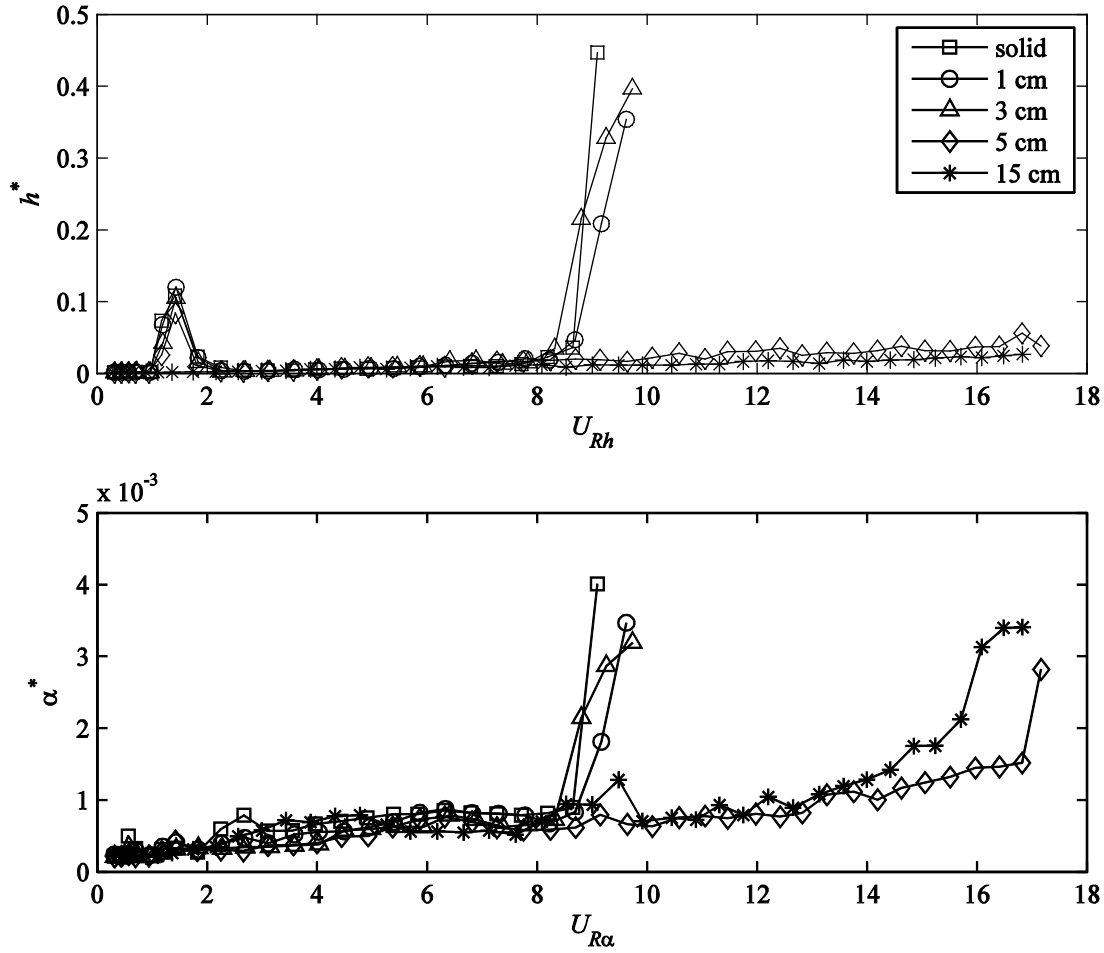

Figure 5. h^* and α^* for the most covered barriers. Circles (○) represent the solid barrier, squares (□) represent configuration 1cm, triangles (Δ) represent configuration 3cm, diamonds (◊) represent configuration 5cm and stars(*) represent configuration 15cm.

It is important to remark that the scale in both graphs is different (bending RMS is two orders of magnitude bigger). This implies that the leading movement in this case is bending. The sudden increase of the response for configurations solid, 1cm and 3cm represent a flutter event. This phenomenon is observed at a reduced wind speed between 8 and 9. There is no big difference in the critical velocity between the configurations that present flutter. The solid configuration has a steeper increase of the response than the other configurations presenting flutter. This observation is enforced by the fact that when flutter appeared, only one measurement could be done, whilst for the other configurations more measurements could be taken at higher wind speeds. When the divergent movement was too large, no further measurements were taken.

The other two configurations present in that figure do not present flutter, even though at high wind speeds the response slowly increases. This phenomenon is related to the buffeting of the bridge. Anyway, this effect is negligible overall. In this case, higher wind speeds have been measured, until the limit of the wind tunnel has been reached.

It is straightforward to conclude that a lower threshold value exists for the gap to obtain a stable bridge deck.

Regarding VIV, it should be pointed out that 4 configurations present it in the bending mode, but the configuration 15cm does not. No torsion VIV was found. The phenomenon is clearly bounded at low velocities. The velocities at which it appears and the amplitude of the response are independent of the configuration. The absence of VIV for configuration 15cm can be explained by the fact that this configuration is less coherent in the spanwise direction. In this configuration, the vortices shed by the covered part and the ones shed by the uncovered part interact and cannot trigger the movement.

It is also significant that the reduced velocity at which it takes place is quite low. This means that the phenomenon could happen at very low wind velocities, producing discomfort for the users, and most dangerous, fatigue loads for the structure. It could even lead to the temporary closure of the bridge for safety reasons.

Figure 6 presents the results for the most opened configurations, from the reference to the 15cm (15cm configuration has been plotted again to use it as a comparison)

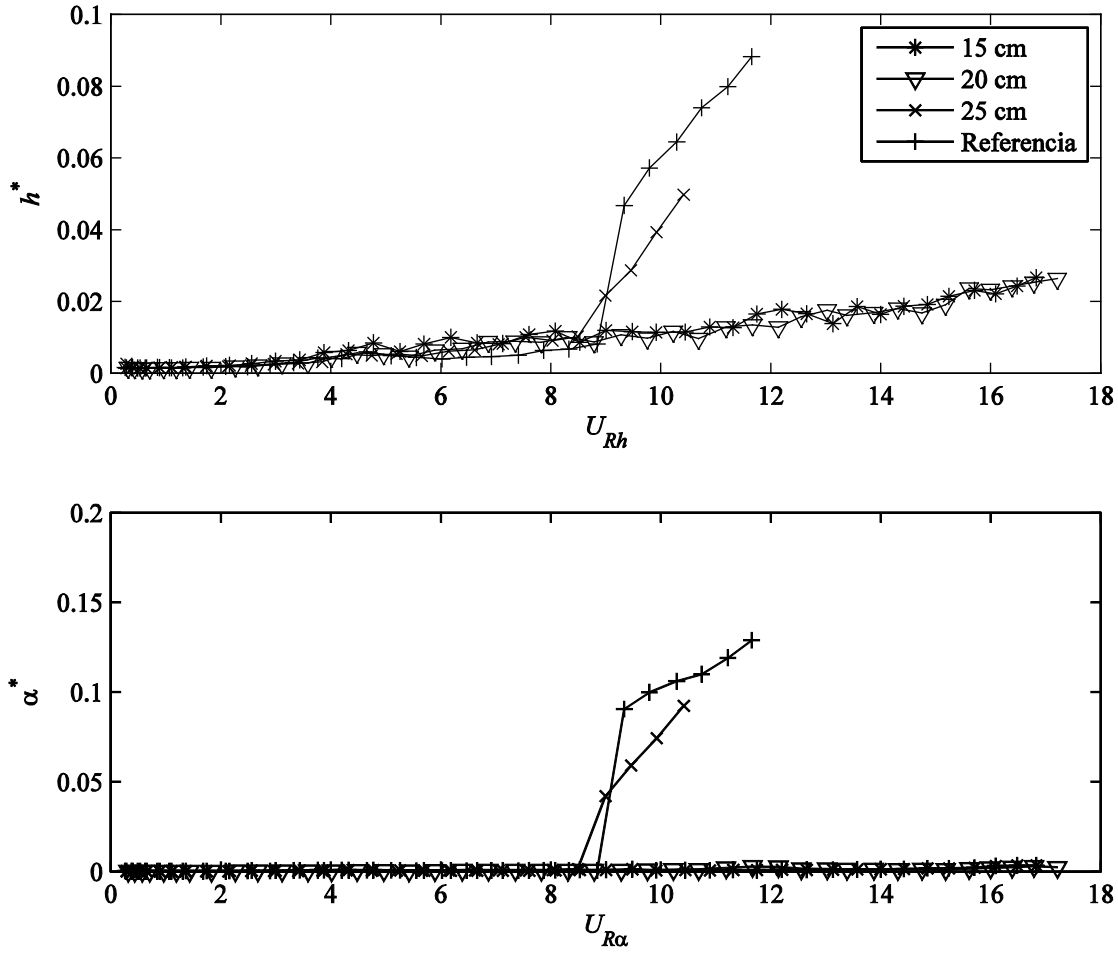

Figure 6. h^* and α^* for the most opened barriers. As in figure 5, stars (*) represent configuration 15cm, inverse triangles (∇) represent configuration 20cm, crosses (x) represent configuration 25cm and pluses (+) represent the reference configuration.

It is clear that torsion is now the leading movement. The scale in the torsional graph is twice the vertical one. In this case, as happened for the most covered barriers, some configurations do not present any instability, namely 15cm and 20cm. The only remarkable wind effect on these barriers is the small increase of the vertical response for high wind speeds. Again, this increase is related to the buffeting.

The other configurations tested, 25cm and the reference barrier, present torsional flutter at reduced wind velocities very similar to the ones at which flutter appeared for the most covered barriers. The increase of the torsional response is steeper for the reference configuration than for the 25cm configuration. Even though flutter is torsional, some vertical response is also noticeable. After watching figure 6, it can also be said that an upper threshold value also exists for the gap to get a stable deck.

No VIV was noticed, neither in bending nor in torsion movement. This may appear as a contradiction to what was said before, that spanwise coherence is a factor that can promote VIV. This apparent contradiction can be explained by two facts. First one is that the vortices shed by the deck may not contain enough energy to trigger the movement. When the barriers were covered, the air flow was facing a thicker object, and bigger vortices were shed to the flow. As now barriers are uncovered, shed vortices are smaller and cannot start the motion. The interaction between the vortices shed by the deck and the smaller vortices shed in the flow by the horizontal elements of the barrier is the other fact that could explain the lack of VIV. This interaction can weaken the bigger vortices, and therefore avoid the motion of the bridge.

CONCLUSIONS

Wind barriers are very useful to protect the pedestrians crossing footbridges, but their design must be very precise to avoid aeroelastic phenomena. Wind tunnel tests have been proved as a key tool to study the stability of a certain bridge configuration. Some conclusions can be extracted:

1.- Porosity of the wall has a great influence on the stability or instability of a given deck. Not only the porosity value, but also its distribution.

2.- A single bridge deck can suffer from different instabilities depending on the wind barrier placed.

3.- The rupture of the spanwise coherence of the barrier is desired to obtain a more stable bridge. The interaction between different size vortices also helps to stabilize the deck.

4.- For a certain range of sizes of the gap the deck is totally stable (neither VIV nor flutter are present). The covered barriers suffer both bending VIV and flutter, whilst the reference barrier suffers torsional flutter. In this case, configurations 15cm and 20cm are suggested

REFERENCES

Aslan, H. & Starossek, U., 2008. Passive control of bridge deck flutter using tuned mass dampers and control surfaces. In *European Conference on Structural Dynamics*.

Chen, Z.Q. et al., 2012. Flutter, Galloping, and Vortex-Induced Vibrations of H-Section Hangers. *Journal of bridge engineering*, 17(3), pp.500–508.

Cluni, F., Gusella, V. & Ubertini, F., 2007. A parametric investigation of wind-induced cable fatigue. *Engineering Structures*, 29(11), pp.3094–3105. Available at: http://linkinghub.elsevier.com/retrieve/pii/S0141029607000910 [Accessed April 9, 2014].

Jones, N.P. et al., 1995. The effect of section model details on aeroelastic parameters. *Journal of Wind Engineering and Industrial Aerodynamics*, 55, pp.45–53.

Kobayashi, H. & Nagaoka, H., 1992. Active control of flutter of a suspension bridge. *Journal of Wind Engineering and Industrial Aerodynamics*, 41-44, pp.143–151.

Matsumoto, M., 1999. Vortex shedding of bluff bodies: a review. *Journal of Fluids and Structures*, 13, pp.791–811. Available at: http://www.sciencedirect.com/science/article/pii/S0889974699902499 [Accessed March 26, 2014].

Matsumoto, Masaru et al., 2003. Effects of aerodynamic interferences between heaving and torsional vibration of bridge decks: the case of Tacoma Narrows Bridge. *Journal of Wind Engineering and Industrial Aerodynamics*, 91, pp.1547–1557. Available at: http://linkinghub.elsevier.com/retrieve/pii/S016761050300120X [Accessed March 26, 2013].

Simiu, E. & Scanlan, Robert H., 1996. *Wind effects on structures*, New York, USA: John Wiley & Sons.

Yoshimura, T. et al., 1997. Half-circular and half-elliptic edge modifications for increasing aerodynamic stability of stress-ribbon pedestrian bridges. *Journal of Wind Engineering and Industrial Aerodynamics*, 69-71, pp.861–870. Available at: http://linkinghub.elsevier.com/retrieve/pii/S0167610597002122.